Contrasting weathering dynamics within continents during the past glacial cycles

Yibo Yang[1*], Albert Galy[2], Xiaomin Fang[1],

[1] Institute of Tibetan Plateau Research, Chinese Academy of Sciences, Beijing, *yangyibo@itpcas.ac.cn; [2] CRPG, UMR7358, CNRS, Université de Lorraine, Nancy;

Outlook

Chemical weathering of the continental rocks exerts a dominant force on atmospheric CO_2 levels and global climate. How continental weathering works during the Quaternary cooling on glacial-interglacial scales is still poorly understood. Here we reconstructed continental weathering history over the past 800 kyr in a High-Mountain Asia catchment impacted by glaciers (**Figure 1**). The lake water $^{87}Sr/^{86}Sr$ ratio, a proxy of catchment weathering, was higher during glacials and cold stages in interglacials, and lower during interglacials (**Figure 2**). This rise in $^{87}Sr/^{86}Sr$ ratio is assumed to be caused by a glacier-forced release of radiogenic strontium from reactive minerals. Conversely, $^{87}Sr/^{86}Sr$ ratio of weathering solution in the Chinese Loess Plateau, a non-glaciated region, displayed lower values during glacials (loess formation) and higher values during interglacials (paleosol formation), which is modulated by temperature dominance of mineral weathering rate (**Figure 3**). Such contrasting weathering dynamics in glaciated and non-glaciated regions suggest that the $^{87}Sr/^{86}Sr$ ratios of river water delivered into the ocean will be greatly buffered by the contrasting Sr release regimes within continents. This process may limit seawater $^{87}Sr/^{86}Sr$variation within a narrow range on glacial-interglacial time scales and provide a novel indicator for tracing the onset of glacial development during the deep past.

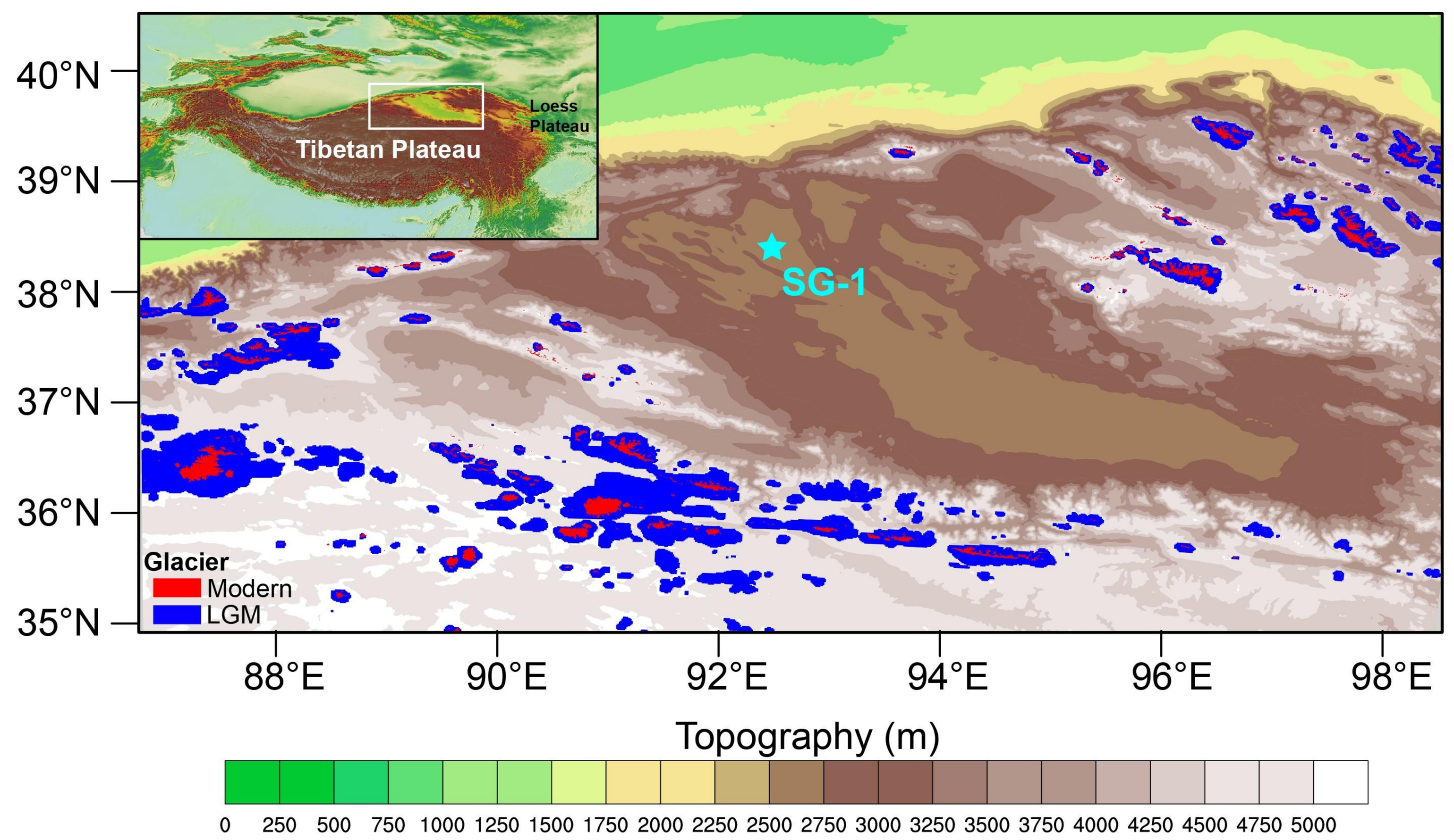

Figure 1 Modern and LGM glacier distribution in the catchment of the Qaidam Basin. The red area marks the modern glacier distribution according to observations. The blue area is modelled LGM glaciers extent with PMIP3 forcing after a decline of 50% in precipitation and of 6° C in temperature (Yan et al., 2018).

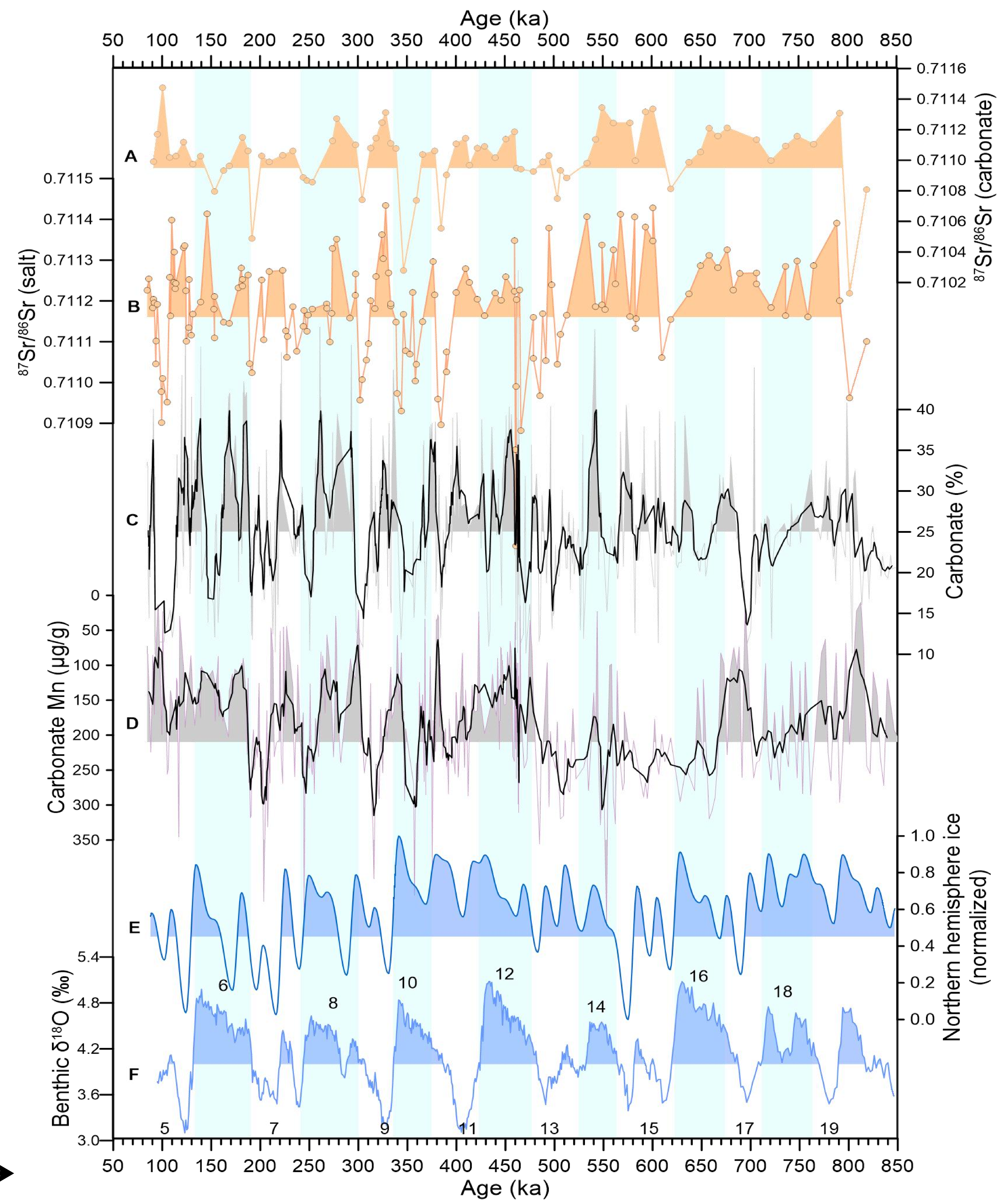

Figure 2 Lake water $^{87}Sr/^{86}Sr$ record in the western Qaidam Basin. (A) SG-1 core carbonate $^{87}Sr/^{86}Sr$ record. (B) SG-1 core salt $^{87}Sr/^{86}Sr$ record (water-soluble salt in this study and gypsum from Li et al., 2021). (C) SG-1 core carbonate content (Han et al., 2020). SG-1 core carbonate Mn content (Yang et al., 2017 and this study). (E) Northern Hemisphere modelled ice volume (Imbrie and Imbrie, 1980). (F) Benthic δ18O stack (Lisiecki and Raymo, 2005). Numbers indicate MIS. The shaded areas indicate glacials. Bold lines show 5-point running averages of raw data in (C) and (D).

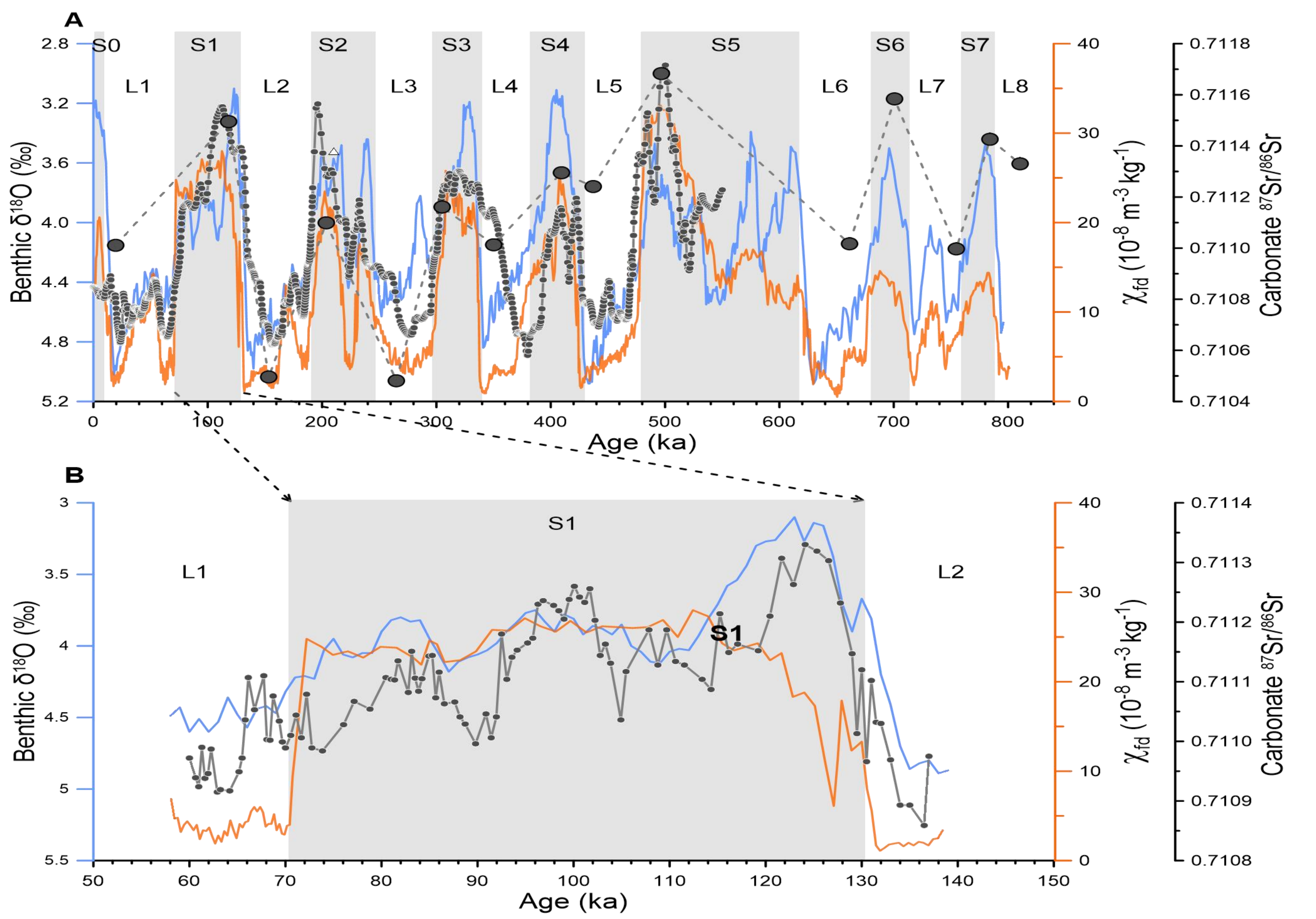

Figure 3 Soil solution $^{87}Sr/^{86}Sr$ records in the Chinese Loess Plateau. (A) $^{87}Sr/^{86}Sr$ ratios of bulk carbonate in each loess and paleosol layers during the past eight glacial cycles (large dots, Rao et al., 2008) as well as $^{87}Sr/^{86}Sr$ ratos of microcodium (biological authigenic carbonate) (small gray dots, Li et al. 2023) with comparison with frequency dependent magnetic susceptibility (χ_{fd}) (Hao et al., 2012), a sensitive soil iron mineral weathering proxy in the Chinese Loess Plateau, and benthic $\delta^{18}O$ (Lisiecki and Raymo, 2005). (B) A high-resolution microcodium $^{87}Sr/^{86}Sr$ record of at the last glacial cycle (Li et al., 2021). The shaded areas indicate major loess (L) and paleosol (S) units.